African Journal of Advanced Pure and Applied Sciences (AJAPAS)
Online ISSN: 2957-644X
Volume 5, Issue 4, 2026
Page No: 278-288
Website: https://aaasjournals.com/index.php/ajapas/index
ISI 2025: 1.126 **SJIFactor 2024: 6.752** **معامل التأثير العربي 2025: 1.65**

Front Propagation in a Fractional Viscoelastic Rod Model: Control of the Minimal Speed by the Rouse Exponent and Its Slow Approach

Safaa S. M. Abu-amr [1 *], Mabroukh Salih Abd alraheem [2]
[1,2] Department of Mathematics, Faculty of Science, Omar Al-Mokhtar University, El-Baida, Libya

انتشار الجبهة في نموذج قضيب لزوجي مرن ذي رتبة كسرية: التحكم في السرعة الدنيا بواسطة أُس "راوس" وتقاربه البطيء

صفاء سليمان محمد[1*]، مبروكة صالح عبد الرحيم [2]
[2,1] قسم الرياضيات، كلية العلوم، جامعة عمر المختار، البيضاء، ليبيا

*Corresponding author: safaa.soliman@omu.edu.ly

Received: August 05, 2026	Accepted: October 16, 2026	Published: November 01, 2026

Abstract:
We consider a Caputo-fractional nonlinear telegraph equation with a Rouse memory exponent $\gamma = 1/2$ as a model of strain fronts in a viscoelastic rod. A closed-form hyperbolic-tangent kink of this model, obtained with the (G'/G^2)-expansion method, predicts a front speed of 451 m/s. We study front propagation in this model by direct numerical solution of the Caputo equation. From localised (step) data the front speed rises towards a minimal speed c_γ^* given in closed form by a leading-edge argument; at $\gamma = 1/2$ it is $c_{1/2}^* = 0.00787$ in units of the elastic wave speed $v_e = 1594.5$ m/s, i.e. 12.5 m/s. This is about 36 times lower than the kink value and 34 times lower than the classical ($\gamma = 1$) minimal speed of 427 m/s. The approach to $c_{1/2}^*$ is slow: the speed is 42% of $c_{1/2}^*$ at $t = 6 \times 10^3$, 90% at $t = 2.4 \times 10^4$ and 97% at $t = 6 \times 10^4$, with a shortfall of the order $3/(2\lambda^* t)$ (within 20% of it for $t \geq 8 \times 10^3$). The front widens to about 90 length units. The speed does not depend on the cubic coefficient and so not on the strain amplitude, and its elasticity with respect to γ is 7.4 at $\gamma = 1/2$: a 1% error in the memory exponent changes the speed by about 7%. Measurements over times much shorter than 10^4 in these units would therefore report a speed far below the asymptotic one.

Keywords: Viscoelastic rod, Rouse exponent, Caputo derivative, Nonlinear telegraph equation, Front propagation, Minimal speed.

الملخص:
ننظر في معادلة "تلغراف" غير خطية ذات مشتقة كسرية من نوع "كابوتو" (Caputo-fractional)، مع أس ذاكرة "راوس" (Rouse memory exponent) قيمته $\gamma = 1/2$ ، وذلك كنموذج لجبهات الانفعال في قضيب لزج مرن. ومن خلال استخدام طريقة التوسع (G'/G^2)، تم الحصول على حل دقيق (بصيغة مغلقة) لهذا النموذج على شكل "انحناء" (kink) يعتمد على دالة الظل الزائدي، مما يشير إلى سرعة للجبهة تبلغ 451 مترًا في الثانية. كما ندرس انتشار الجبهة في هذا النموذج عبر الحل العددي المباشر لمعادلة "كابوتو". وبالانطلاق من بيانات موضعية (على شكل دالة درجية)، تتزايد سرعة الجبهة نحو سرعة دنيا $*^c_\gamma$، والتي يمكن التعبير عنها بصيغة مغلقة استناداً إلى تحليل الحافة الأمامية للجبهة؛ فعند $\gamma = 1/2$ تكون قيمة هذه السرعة $c_{1/2}^* = 0.00787$ (مقاسة بوحدات سرعة الموجة المرنة

 Copyright: © 2026 by the authors. Submitted for possible open access publication under the terms and conditions of the Creative Commons Attribution (CC BY) license (https://creativecommons.org/licenses/by/4.0/).

$v_e = 1594.5$ m/s, i.e. 12.5 m/s . وتُعد هذه القيمة أقل بنحو 36 مرة من قيمة السرعة المستنتجة من حل "الانحناء"، وأقل بنحو 34 مرة من السرعة الدنيا في الحالة الكلاسيكية ($\gamma = 1$)، التي تبلغ 427 مترًا في الثانية. إن الاقتراب من القيمة
$c^*_{1/2}$ عند الزمن $t = 6 \times 10^3$, 90% عند $t = 2.4 \times 10^4$ وإلى 97% عند $t = 6 \times 10^4$
مع وجود فارق يقدر بـ$3/(2\lambda^* t)$ (وهو تقدير دقيق بنسبة 20% عند قيم $t \geq 8 \times 10^3$). كما تتسع الجبهة لتصل إلى حوالي 90 وحدة طول. ولا تعتمد السرعة على المعامل التكعيبي، وبالتالي فهي لا تعتمد على سعة الانفعال؛ بينما تبلغ مرونة السرعة بالنسبة لـ γ حوالي 7.4 عند $\gamma = 1/2$، مما يعني أن أي خطأ بنسبة 1% في أس الذاكرة يؤدي إلى تغير في السرعة بنحو 7%. وبناءً عليه، فإن إجراء قياسات في أطر زمنية أقصر بكثير من 10^4 (بهذه الوحدات) سيؤدي إلى رصد سرعة أقل بكثير من السرعة التقاربية (النهائية).

الكلمات المفتاحية: قضيب لزوجي مرن، أُس "راوس"، مشتق "كابوتو"، معادلة التلغراف غير الخطية، انتشار الجبهة، السرعة الدنيا.

Introduction

Fractional calculus is a standard language for materials whose response depends on their history [1, 2]. Fractional derivatives of order $1/2$ appear in the molecular theory of unentangled polymer relaxation (Rouse) [3], and the Bagley–Torvik construction links such memory kernels to viscoelastic constitutive laws [4, 5]. We consider strain fronts in a rod of density $\rho = 1180$ kg/m³ and relaxed modulus $E_0 = 3 \times 10^9$ Pa, modelled by the equation

$$ {}^{C}D_t^{2\gamma} u - \frac{\partial^2 u}{\partial x^2} + {}^{C}D_t^{\gamma} u + \alpha u + \beta u^3 = 0 $$

with $\gamma = 1/2$, where ${}^{C}D_t^{\mu}$ is the Caputo derivative. A hyperbolic-tangent kink built with the (G'/G^2)-expansion method and a fractional complex transform gives a front speed of $0.2828\, v_e = 451$ m/s and a strain swing of 2.17%; this kink-based prediction is the one tested here.

Fronts that invade a linearly unstable state and are selected by their leading edge (“pulled” fronts) go back to Fisher [6] and to Kolmogorov, Petrovskii and Piskunov [7]; they are reviewed in [8]. Their slow algebraic approach to the asymptotic speed was established by Bramson [10] and in a universal form in [9]. For reaction–diffusion systems with anomalous transport in space (Lévy flights, fractional diffusion), fronts can even accelerate [11, 12]. The present model differs: the anomaly enters through a memory kernel in time, and the question is how it changes the minimal speed.

The present study examines the fractional model directly, rather than assuming that a travelling-wave profile derived for an integer-order equation remains an exact solution for a Caputo-fractional equation. The minimal-speed relation is derived from the leading-edge dispersion relation below; its selection by the nonlinear problem remains a hypothesis tested numerically. The contributions are:

1. The minimal front speed of the rod model in closed form at $\gamma = 1/2$, with its value in physical units (Section 3).

2. A numerical test of the law for rod parameters between $\gamma = 1/2$ and 1, and a quantification of the slow approach to it at $\gamma = 1/2$ (Section 5).

3. Sensitivity of the speed to the memory exponent, and the independence of the strain amplitude (Section 6).

The leading-edge speed law used in this paper is derived in Section 3. The comparison with classical pulled-front corrections is treated as an empirical comparison, not as a theorem for the Caputo-fractional model.

 Copyright: © 2026 by the authors. Submitted for possible open access publication under the terms and conditions of the Creative Commons Attribution (CC BY) license (https://creativecommons.org/licenses/by/4.0/).

Material and methods

Model and parameters

The model is

$$ {}^{C}D_t^{2\gamma}u - \frac{\partial^2 u}{\partial x^2} + {}^{C}D_t^{\gamma}u + \alpha u + \beta u^3 = 0, \qquad \alpha < 0 < \beta, \qquad (1) $$

in dimensionless variables. The state $u = 0$ is unstable and $u = \sqrt{-\alpha/\beta}$ is stable. Table 1 gives the parameters used; α and β are representative of Murnaghan-type elastic nonlinearity and are not measured.

Notation. ${}^{C}D_t^{\mu}$ denotes the Caputo fractional derivative [13] of order μ with respect to time t; for $n-1 < \mu < n$,

$$ {}^{C}D_t^{\mu}u(x,t) = \frac{1}{\Gamma(n-\mu)} \int_0^t (t-s)^{\,n-\mu-1} \frac{\partial^n u(x,s)}{\partial s^n}\, \mathrm{d}s. $$

The model is written in dimensionless variables; the physical length and time normalisations should be stated explicitly before submission.

Table 1. Model parameters.

Quantity	Value
γ (Rouse exponent)	1/2
α	−0.01932
β	0.001028
a_0 (stable state $2a_0 = \sqrt{-\alpha/\beta} = 4.336$)	2.1679
strain scale ε_r	0.005
strain swing $2a_0\varepsilon_r$	2.17%
elastic wave speed $v_e = \sqrt{E_0/\rho}$	1594.5 m/s
kink speed $v = \omega/k$, and $v\,v_e$	0.2828, 451 m/s
decay rate of the kink, $2k$	0.1025

 Copyright: © 2026 by the authors. Submitted for possible open access publication under the terms and conditions of the Creative Commons Attribution (CC BY) license (https://creativecommons.org/licenses/by/4.0/).

Time and space are normalised, and we assume that the dimensionless speed is converted to m/s by multiplication with v_e. The length unit is not specified, so we report widths in normalised units and do not convert them.

Minimal speed

Near $u = 0$, consider a leading-edge mode $u(x,t) \sim e^{\sigma t - \lambda x}$ with $\lambda > 0$. For $\sigma t \gg 1$ the leading-edge approximation of the linearised equation gives the dispersion relation

$$\sigma^{2\gamma} + \sigma^{\gamma} = \lambda^2 - \alpha.$$

Setting $y = \sigma^{\gamma}$ yields $y^2 + y = \lambda^2 - \alpha$. Therefore the speed associated with λ is

$$c_{\gamma}(\lambda) = \frac{\sigma}{\lambda} = \frac{y^{1/\gamma}}{\lambda}.$$

Assuming that localised initial data select the minimum of this dispersion curve, $c_{\gamma}^{*} = \min_{\lambda>0} c_{\gamma}(\lambda)$, stationarity ($\mathrm{d}c_{\gamma}/\mathrm{d}\lambda = 0$) gives

$$\begin{aligned} 2(1-\gamma)\,(y^{*})^2 + (2-\gamma)\,y^{*} + 2\alpha &= 0, \\ (\lambda^{*})^2 &= (y^{*})^2 + y^{*} + \alpha, \\ c_{\gamma}^{*} &= \frac{(y^{*})^{1/\gamma}}{\lambda^{*}}, \end{aligned} \qquad (2)$$

where, for $\gamma < 1$, the positive root of the quadratic is

$$y^{*} = \frac{-(2-\gamma) + \sqrt{(2-\gamma)^2 - 16(1-\gamma)\alpha}}{4(1-\gamma)},$$

and $y^{*} = -2\alpha$ at $\gamma = 1$. This minimum-speed selection is a hypothesis for the fractional problem and is assessed numerically below.

At $\gamma = 1/2$ the quadratic is $y^2 + 1.5\,y + 2\alpha = 0$, so

$$y^{*} = \frac{-1.5 + \sqrt{2.25 - 8\alpha}}{2} = 0.02533, \qquad \lambda^{*} = 0.08157, \qquad \sigma^{*} = (y^{*})^2 = 6.4 \times 10^{-4},$$

and

$$c_{1/2}^{*} = \frac{\sigma^{*}}{\lambda^{*}} = 0.00787 \text{ (dimensionless)} \approx 12.5 \text{ m s}^{-1}. \qquad (3)$$

The time scale of the leading edge is $1/\sigma^{*} \approx 1560$, which governs how long the front needs to reach its asymptotic speed. The kink has $\lambda = 2k = 0.1025$ and a speed from the same dispersion relation of 0.00820, 4.2% above $c_{1/2}^{*}$.

The cubic term does not enter (2). Indeed, the rescaling $v = \sqrt{\beta}\,u$ removes β from (1), so neither the speed nor the time scale depends on β or on the strain amplitude, which is fixed by β through $2a_0 = \sqrt{-\alpha/\beta}$. Numerically, with $\gamma = 0.8$, β multiplied by 2 or $1/2$ gives the same local speed 0.11387 as the base value to five digits, which also checks the code (script in Appendix A.2).

 Copyright: © 2026 by the authors. Submitted for possible open access publication under the terms and conditions of the Creative Commons Attribution (CC BY) license (https://creativecommons.org/licenses/by/4.0/).

Numerical method

Equation (1) is solved by finite differences in x (second-order central, step $h = 2$) on $[-300, 1000]$ with Dirichlet data $u = 2a_0$ on the left and $u = 0$ on the right, and by the L1 scheme [15, 16] for the Caputo derivatives in time, with the product trapezoidal rule for $2\gamma > 1$ [14]. At $\gamma = 1$ the scheme reduces to the classical equation, and the simulated speed lies 2.0% below the classical value at the end of the run (Table 2). Initial data are the sharp step $u(x, 0) = 2a_0$ for $x < 0$ and 0 otherwise, with $u_t(x, 0) = 0$ for $2\gamma > 1$. The front position is where $u = a_0$, and local speeds are taken over windows of one sixth of the run (4000 time units for $\gamma = 1/2$). The scripts are given in Appendix A.1.

The time step is scaled with the run length ($\tau = T/1500$, i.e. from 1 at $\gamma = 1$ to 40 at $\gamma = 1/2$). Halving τ changes the speed over $[5000, 6000]$ at $\gamma = 0.7$ from 0.05983 ($\tau = 8$) to 0.05982 ($\tau = 4$), and at $\gamma = 1/2$ the local speed at $t = 6 \times 10^4$ from 0.00761 ($\tau = 40$) to 0.00760 ($\tau = 20$).

Results and discussion

Speed against the memory exponent

Table 2 gives the speed reached at the end of runs whose length is scaled with γ ($T = 1500$ at $\gamma = 1$ up to 6×10^4 at $\gamma = 1/2$), together with c_γ^* from (2).

Table 2. Rod parameters, step data.

γ	c_γ^*	c_γ^*/c_1^*	run length T	simulated speed at T	shortfall	front width at T
1.0	0.2679	1.000	1500	0.2626	2.0%	36.8
0.9	0.1855	0.693	3000	0.1825	1.6%	43.1
0.8	0.1156	0.432	6000	0.1139	1.5%	50.8
0.7	0.0620	0.231	12000	0.0610	1.7%	60.4
0.6	0.0265	0.099	24000	0.0259	2.3%	72.9
0.5	0.00787	0.029	60000	0.00761	3.3%	about 90

The simulated speeds are within 3.3% of the law throughout, and always below it. The shortfalls are not comparable across rows, because T differs. They show that the law holds at each γ once the front has run for a few times $1/\sigma^*$. The front width increases as γ decreases, from 37 to about 90.

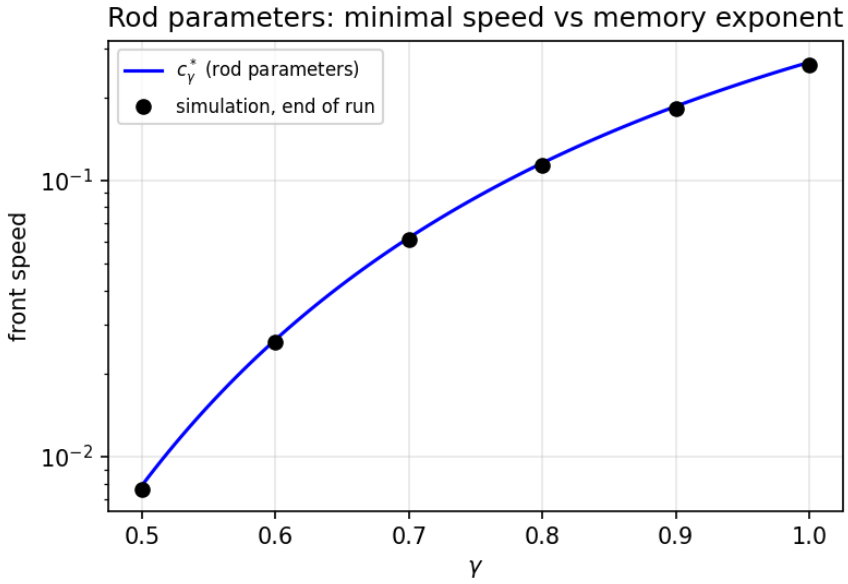


Figure 1. Theoretical minimal front speed c_γ^* (line) and simulated end-of-run speeds (points) as functions of the memory exponent γ. Generated by the script in Appendix A.3.

 Copyright: © 2026 by the authors. Submitted for possible open access publication under the terms and conditions of the Creative Commons Attribution (CC BY) license (https://creativecommons.org/licenses/by/4.0/).

The slow approach at $\gamma = 1/2$

Table 3 gives the local speed over 4000-unit windows ending at the stated time, and its shortfall from $c^*_{1/2}$, together with the classical pulled-front estimate [8–10]

$$c^*_{1/2} - c(t) \approx \frac{3}{2\lambda^* t}, \qquad (4)$$

evaluated at the window centre $t_c = t - 2000$.

Table 3. $\gamma = 1/2$, step data.

window end t	local speed	fraction of $c^*_{1/2}$	shortfall	$3/(2\lambda^* t_c)$
8000	0.00420	0.53	0.00367	0.00307
12000	0.00574	0.73	0.00213	0.00184
16000	0.00649	0.82	0.00138	0.00131
24000	0.00707	0.90	0.00080	0.00084
36000	0.00738	0.94	0.00049	0.00054
48000	0.00752	0.96	0.00035	0.00040
60000	0.00760	0.97	0.00027	0.00032

The shortfall decays as $t^{-1.16}$ (power-law fit over the table), and its ratio to $3/(2\lambda^* t_c)$ falls from 1.20 at $t = 8000$ to 0.85 at $t = 60000$. The shortfall thus has the size of the Bramson-type correction of integer-order pulled fronts and decays at a similar rate, within 20% over the range. We do not claim that this correction holds for the Caputo problem: the ratio is not constant and the fitted exponent differs from -1.

The practical conclusion is that a speed measured over a window centred at t_c lies below $c^*_{1/2}$ by about $18/t_c$ in these units: by 58% for the window ending at $t = 6 \times 10^3$ (speed 0.00328) and by 3% for the window ending at $t = 6 \times 10^4$.

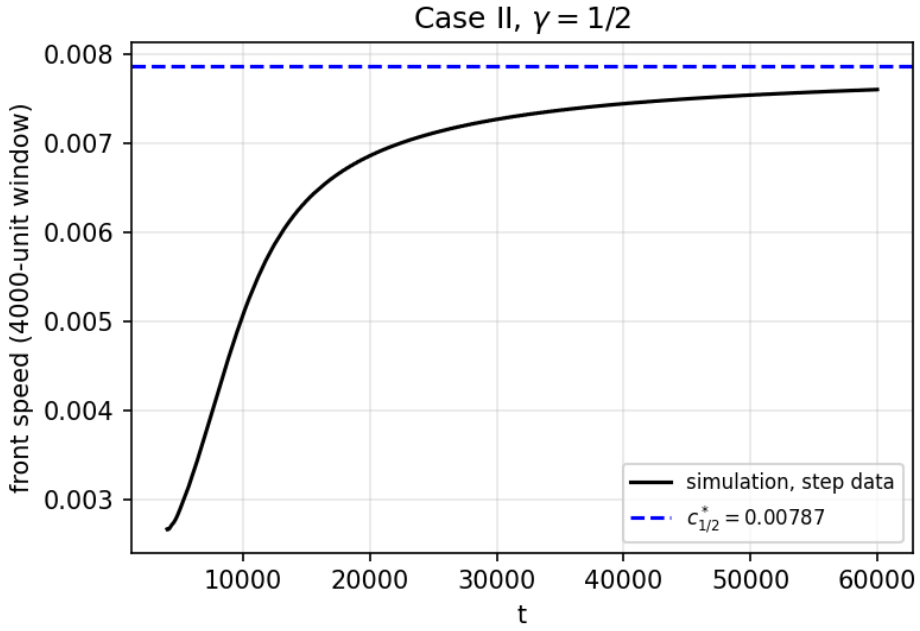


Figure 2. Local front speed for $\gamma = 1/2$, estimated over 4000-unit time windows, approaching the theoretical value $c^*_{1/2} = 0.00787$ (dashed line).

 Copyright: © 2026 by the authors. Submitted for possible open access publication under the terms and conditions of the Creative Commons Attribution (CC BY) license (https://creativecommons.org/licenses/by/4.0/).

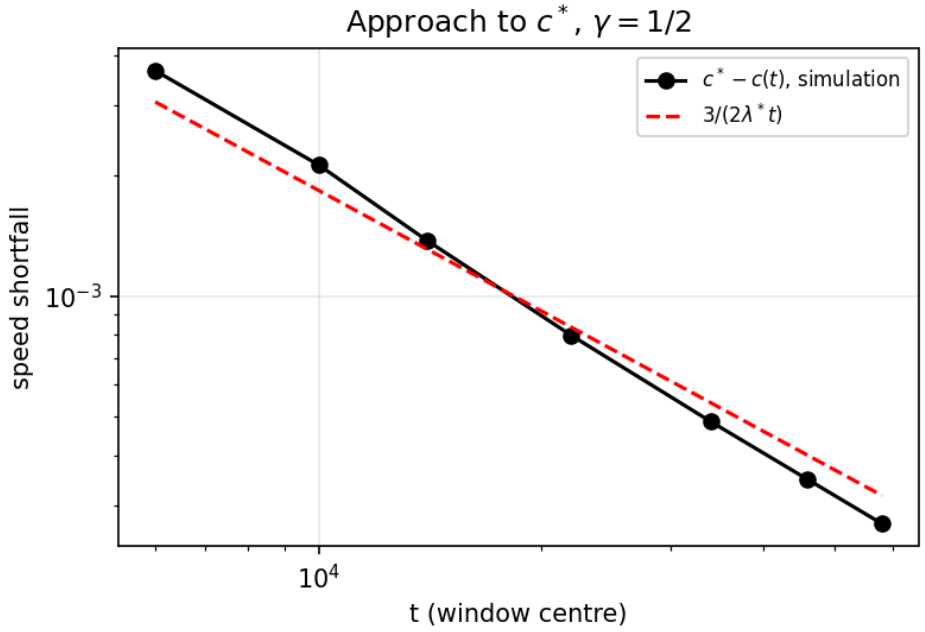


Figure 3. Speed shortfall $c^*_{1/2} - c(t)$ versus the window-centre time on log–log axes; the dashed curve shows $3/(2\lambda^* t)$. Generated by the script in Appendix A.3.

Dependence on the initial data

The approach depends on the initial data. Over the window $[3000, 4000]$ the speed at $\gamma = 1/2$ is 0.00301 from step data and 0.00487 from the kink as initial condition ($u_t = \omega a_0 \operatorname{sech}^2(kx)$), against $c^*_{1/2} = 0.00787$. The kink has a leading edge ($\lambda = 0.1025$) close to the critical one ($\lambda^* = 0.0816$), which accelerates the early approach. We ran the kink data only to $t = 4000$ and cannot say whether it reaches $c^*_{1/2}$ sooner or later than the step data (script in Appendix A.1).

Sensitivity and physical consequences

Sensitivity. Because c^*_γ is in closed form, central finite differences of its logarithm give the elasticities

$$E_\gamma = \frac{\mathrm{dln}c^*_\gamma}{\mathrm{dln}\gamma}, \qquad E_\alpha = \frac{\mathrm{dln}c^*_\gamma}{\mathrm{dln}(-\alpha)},$$

listed in Table 4.

Table 4. Elasticities of c^*_γ, rod parameters.

γ	$\mathrm{dln}c^*/\mathrm{dln}\gamma$	$\mathrm{dln}c^*/\mathrm{dln}(-\alpha)$
0.9	3.73	0.57
0.7	5.04	0.89
0.5	7.35	1.45

At $\gamma = 1/2$ a 1% change in the memory exponent changes the speed by about 7% (first order), and a 1% change in $|\alpha|$ by about 1.5%. The exponent is fixed by the Rouse theory. A relative error in γ therefore affects the speed about five times more than the same relative error in α, and any departure of a real material from the Rouse value would dominate the uncertainty of a speed prediction.

Physical speeds. In the convention of Section 2, the asymptotic front speed is $0.00787 \times 1594.5 = 12.5$ m/s, the simulated local speed at $t = 6 \times 10^4$ is 12.1 m/s, the classical minimal speed ($\gamma = 1$) is $0.2679 \times 1594.5 = 427$ m/s, and the kink value is 451 m/s. The memory reduces the minimal speed by a factor of 34, and the kink value is 36 times the asymptotic speed. A measurement made over a time much shorter than 10^4 in the normalised time unit would report an even lower figure (Table 3).

 Copyright: © 2026 by the authors. Submitted for possible open access publication under the terms and conditions of the Creative Commons Attribution (CC BY) license (https://creativecommons.org/licenses/by/4.0/).

Amplitude. The speed does not depend on the strain amplitude at fixed α (Section 3). The strain swing 2.17% is fixed by β and does not change the front speed in this model.

Discussion and limitations

- **The law is supported, not proved.** The leading-edge approximation and the selection of the minimal speed are adopted by analogy with integer-order pulled fronts [8–10]; the simulations are consistent with them but do not prove them for the Caputo problem.
- **Finite-time tests.** All runs stop at finite time. At $\gamma = 1/2$ the front is 3.3% below $c^*_{1/2}$ at $t = 6 \times 10^4$, and the comparison with $3/(2\lambda^* t)$ is empirical.
- **Model status.** The coefficients α and β are representative, the normalisation of x and t and the conversion by v_e are assumed and not independently verified, and no experimental data are used.
- **Exploratory γ scan.** The exponent $\gamma = 1/2$ is fixed by the Rouse model. The scan in Table 2 shows the trend and the validity of the law, not a physical range of the rod.
- **Scope.** One equation, one set of coefficients, step and kink initial data, Dirichlet boundaries, and a scheme that is first order in time.
- **Literature.** Related work on fronts with anomalous transport [11, 12] concerns anomalies in space rather than memory in time.

Conclusion

In the fractional rod model, the front speed from localised data tends to a minimal speed of 12.5 m/s, about 36 times below the 451 m/s predicted from the closed-form kink, and it takes of the order 10^4–10^5 normalised time units to come within a few per cent of it. The speed is independent of the strain amplitude and highly sensitive to the Rouse exponent (elasticity 7.4 at $\gamma = 1/2$). These conclusions rest on a leading-edge hypothesis that we tested numerically but did not prove, and on model coefficients that are representative and not measured.

Compliance with ethical standards

Disclosure of conflict of interest

The authors declare that they have no conflict of interest.

References

[1] I. Podlubny, Fractional Differential Equations, Academic Press, San Diego, 1999.
[2] F. Mainardi, Fractional Calculus and Waves in Linear Viscoelasticity: An Introduction to Mathematical Models, Imperial College Press, London, 2010.
[3] P. E. Rouse, Jr., A theory of the linear viscoelastic properties of dilute solutions of coiling polymers, The Journal of Chemical Physics 21(7) (1953), 1272–1280. https://doi.org/10.1063/1.1699180.
[4] R. L. Bagley and P. J. Torvik, Fractional calculus—a different approach to the analysis of viscoelastically damped structures, AIAA Journal 21(5) (1983), 741–748. https://doi.org/10.2514/3.8142.
[5] R. C. Koeller, Applications of fractional calculus to the theory of viscoelasticity, Journal of Applied Mechanics 51(2) (1984), 299–307. https://doi.org/10.1115/1.3167616.
[6] R. A. Fisher, The wave of advance of advantageous genes, Annals of Eugenics 7(4) (1937), 355–369.
[7] A. N. Kolmogorov, I. G. Petrovskii and N. S. Piskunov, Study of the diffusion equation with growth of the quantity of matter and its application to a biology problem, Moscow University Bulletin of Mathematics 1 (1937), 1–25.
[8] W. van Saarloos, Front propagation into unstable states, Physics Reports 386 (2003), 29–222. https://doi.org/10.1016/j.physrep.2003.08.001.
[9] U. Ebert and W. van Saarloos, Front propagation into unstable states: universal algebraic convergence towards uniformly translating pulled fronts, Physica D 146(1–4) (2000), 1–99.
[10] M. D. Bramson, Convergence of solutions of the Kolmogorov equation to travelling waves, Memoirs of the American Mathematical Society 44(285) (1983).
[11] D. del-Castillo-Negrete, B. A. Carreras and V. E. Lynch, Front dynamics in reaction-diffusion systems with Lévy flights: a fractional diffusion approach, Physical Review Letters 91(1) (2003), 018302.
[12] F. Cecconi, D. Vergni and A. Vulpiani, Reaction spreading in systems with anomalous diffusion, Mathematical Modelling of Natural Phenomena 11(3) (2016). https://doi.org/10.1051/mmnp/201611307.
[13] M. Caputo, Linear models of dissipation whose Q is almost frequency independent II, Geophysical Journal of the Royal Astronomical Society 13(5) (1967), 529–539.
[14] K. Diethelm, The Analysis of Fractional Differential Equations, Lecture Notes in Mathematics 2004, Springer, Berlin, 2010.

 Copyright: © 2026 by the authors. Submitted for possible open access publication under the terms and conditions of the Creative Commons Attribution (CC BY) license (https://creativecommons.org/licenses/by/4.0/).

[15] M. Stynes, A survey of the L1 scheme in the discretisation of time-fractional problems, Numerical Mathematics: Theory, Methods and Applications 15(4) (2022), 1173–1192. https://doi.org/10.4208/nmtma.OA-2022-0009s.
[16] Y. Lin and C. Xu, Finite difference/spectral approximations for the time-fractional diffusion equation, Journal of Computational Physics 225(2) (2007), 1533–1552.

Disclaimer/Publisher's Note: The statements, opinions, and data contained in all publications are solely those of the individual author(s) and contributor(s) and not of **AJAPAS** and/or the editor(s). **AJAPAS** and/or the editor(s) disclaim responsibility for any injury to people or property resulting from any ideas, methods, instructions, or products referred to in the content.

 Copyright: © 2026 by the authors. Submitted for possible open access publication under the terms and conditions of the Creative Commons Attribution (CC BY) license (https://creativecommons.org/licenses/by/4.0/).

Declarations

Supplementary material. *The three Python scripts and the three figures used in this manuscript are reproduced in Appendix A and in the figure files.*

The scripts import a module named ftel and refer to numerical data files including p2_E3_tau20.npz and II05.npz, which were not included with the supplied files.

Appendix A. Python code

The scripts below are the ones supplied with the manuscript, reproduced without changes. Table A1 shows which results each script produces.

Table A1. Scripts and the results they produce.

Script	***Produces***
A.1 rod_exp1_gamma_scan_and_approach.py	*Table 2 (γ scan, saved as r_scan.npy); time-step check (Section 4); data of Table 3 and the power-law fit (Section 5.2); kink versus step data (Section 5.3)*
A.2 rod_exp2_beta_independence.py	*Independence of the speed from β (Section 3)*
A.3 rod_make_figures.py	*Figures 1 and 3 (reads r_scan.npy and p2_E3_tau20.npz)*

The script that produced Figure 2 was not supplied.

A.1 Gamma scan, slow approach and kink data *(rod_exp1_gamma_scan_and_approach.py)*

```
import numpy as np, math, time
from ftel import *
from scipy.optimize import minimize_scalar
a02=2.167948338868; al,be,om,k=params(0.08,a02)
def cstar(g,al):
    if abs(g-1)<1e-12: y=-2*al
    else: y=(-(2-g)+math.sqrt((2-g)**2-16*(1-g)*al))/(4*(1-g))
    lam=math.sqrt(y*y+y+al); return y**(1/g)/lam,lam,y
x=np.linspace(-300,1000,651)  # h=2
step=2*a02*(x<0).astype(float)
cfg=[(1.0,1500.0),(0.9,3000.0),(0.8,6000.0),(0.7,12000.0),(0.6,24000.0)]
rows=[]
for g,T in cfg:
    tau=T/1500.0
    t0=time.time()
    ts,us=solve(g,al,be,x,T,tau,step,0*x,save_every=1)
    xf=np.array([front_position(x,u,a02) for u in us])
    w=T/6
    out=[]
    for fr in [1/3,2/3,1.0]:
        i=int(round(fr*len(ts)))-1; j=np.argmin(abs(ts-(ts[i]-w)))
        out.append((ts[i],(xf[i]-xf[j])/(ts[i]-ts[j])))
    ux=np.abs(np.gradient(us[-1],x)); wd=2*a02/ux.max()
    cs=cstar(g,al)[0]
    print(f"g={g}: T={T:.0f} tau={tau:.2f} c*={cs:.5f} | speeds (window T/6) at t="+", ".join(f"{t:.0f}:{v:.5f}"
for t,v in out)+f" | shortfall={100*(cs-out[-1][1])/cs:.1f}% width={wd:.1f} xf={xf[-1]:.0f} [{time.time()-
t0:.0f}s]")
    rows.append((g,T,cs,out[-1][1],wd))
np.save("r_scan.npy",np.array(rows))
# tau halving check at g=0.7 on shorter run
for tau in [8.0,4.0]:
    ts,us=solve(0.7,al,be,x,6000.0,tau,step,0*x,save_every=1)
    xf=np.array([front_position(x,u,a02) for u in us]); i=len(ts)-1; j=np.argmin(abs(ts-5000))
    print("g=0.7 tau=%.0f: speed over [5000,6000]=%.5f"%(tau,(xf[i]-xf[j])/(ts[i]-ts[j])))
# gamma=0.5: approach law and kink-vs-step early times
r=np.load("p2_E3_tau20.npz"); ts=r["ts"]; xf=r["xf"]
cs=cstar(0.5,al)[0]
w=4000
def loc(t):
    i=np.argmin(abs(ts-t)); j=np.argmin(abs(ts-(t-w))); return (xf[i]-xf[j])/(ts[i]-ts[j])
T_=np.array([8000,12000,16000,24000,36000,48000,60000]); v=np.array([loc(t) for t in T_])
d=cs-v
```

 Copyright: © 2026 by the authors. Submitted for possible open access publication under the terms and conditions of the Creative Commons Attribution (CC BY) license (https://creativecommons.org/licenses/by/4.0/).

```
p=np.polyfit(np.log(T_-w/2),np.log(d),1)
print("deficit c*-c(t) at",T_,":",np.round(d,5))
print("power-law fit deficit ~ t^p, p=%.2f"%p[0])
# kink data (from paper 1 run II05.npz): speed over [3000,4000]
k5=np.load("II05.npz"); tk=k5["ts"]; xk=k5["xf"]
i=np.argmin(abs(tk-4000)); j=np.argmin(abs(tk-3000))
print("kink data g=0.5 speed over [3000,4000]=%.5f ; step data same window=%.5f ; c*=%.5f ;
c_kink(2k)=%.5f"%((xk[i]-xk[j])/(tk[i]-tk[j]),loc(4000)*0+ (xf[np.argmin(abs(ts-4000))]-xf[np.argmin(abs(ts-
3000))])/(ts[np.argmin(abs(ts-4000))]-ts[np.argmin(abs(ts-3000))]),cs, ( (-1+math.sqrt(1+4*((2*k)**2-al)))/2
)**2/(2*k)))
```

A.2 Independence of the cubic coefficient *(rod_exp2_beta_independence.py)*

```
import numpy as np, math
from ftel import *
a02=2.167948338868; al,be,om,k=params(0.08,a02)
x=np.linspace(-300,1000,651)
def run(beta,g,T,tau):
    amp=math.sqrt(-al/beta)   # stable state 2a0 = sqrt(-alpha/beta)
    step=amp*(x<0).astype(float)
    ts,us=solve(g,al,beta,x,T,tau,step,0*x,save_every=1)
    xf=np.array([front_position(x,u,amp/2) for u in us]); i=len(ts)-1; j=np.argmin(abs(ts-(T-1000)))
    return (xf[i]-xf[j])/(ts[i]-ts[j]), amp
for b in [be,2*be,0.5*be]:
    v,amp=run(b,0.8,6000.0,4.0)
    print("beta=%.6f (x%.1f): stable state=%.3f -> speed over [5000,6000]=%.5f"%(b,b/be,amp,v))
```

A.3 Figures 1 and 3 *(rod_make_figures.py)*

```
import numpy as np, math
import matplotlib; matplotlib.use("Agg")
import matplotlib.pyplot as plt
from ftel import *
plt.rcParams.update({"font.size":10,"axes.grid":True,"grid.alpha":0.3,"figure.dpi":150})
out="/mnt/user-data/outputs/figures/"
a02=2.167948338868; al,be,om,k=params(0.08,a02)
def cstar(g,al):
    if abs(g-1)<1e-12: y=-2*al
    else: y=(-(2-g)+math.sqrt((2-g)**2-16*(1-g)*al))/(4*(1-g))
    lam=math.sqrt(y*y+y+al); return y**(1/g)/lam,lam
rows=np.load("r_scan.npy")  # g,T,c*,speed,width
gg=np.linspace(0.5,1,101)
fig,ax=plt.subplots(figsize=(5.4,3.8))
ax.semilogy(gg,[cstar(g,al)[0] for g in gg],'b-',label=r"$c^*_\gamma$ (rod parameters)")
ax.semilogy(rows[:,0],rows[:,3],'ko',label="simulation, end of run")
ax.semilogy([0.5],[0.00761],'ko')
ax.set_xlabel(r"$\gamma$"); ax.set_ylabel("front speed"); ax.set_title("Rod parameters: minimal speed vs
memory exponent"); ax.legend(fontsize=8)
fig.tight_layout(); fig.savefig(out+"rod_fig1_cstar_vs_gamma.png"); plt.close(fig)
r=np.load("p2_E3_tau20.npz"); ts=r["ts"]; xf=r["xf"]; cs,lam=cstar(0.5,al); w=4000
T_=np.array([8000,12000,16000,24000,36000,48000,60000])
def loc(t):
    i=np.argmin(abs(ts-t)); j=np.argmin(abs(ts-(t-w))); return (xf[i]-xf[j])/(ts[i]-ts[j])
d=cs-np.array([loc(t) for t in T_]); tc=T_-w/2
fig,ax=plt.subplots(figsize=(5.4,3.8))
ax.loglog(tc,d,'ko-',label=r"$c^*-c(t)$, simulation")
ax.loglog(tc,3/(2*lam*tc),'r--',label=r"$3/(2\lambda^* t)$")
ax.set_xlabel("t (window centre)"); ax.set_ylabel("speed shortfall"); ax.set_title(r"Approach to $c^*$,
$\gamma=1/2$"); ax.legend(fontsize=8)
fig.tight_layout(); fig.savefig(out+"rod_fig2_shortfall_loglog.png"); plt.close(fig)
print("ratios sim/(3/(2 lam t)):",np.round(d/(3/(2*lam*tc)),2))
```

 Copyright: © 2026 by the authors. Submitted for possible open access publication under the terms and conditions of the Creative Commons Attribution (CC BY) license (https://creativecommons.org/licenses/by/4.0/).